



Encapsulation of *Leflunomide* (LFD) in a novel niosomal formulation facilitated its delivery to THP-1 monocytic cells and enhanced *Aryl hydrocarbon receptor* (AhR) nuclear translocation and activation

Mahsa Hasani¹ · Neda Abbaspour Sani¹ · Behnaz Khodabakhshi² · Mehdi Sheikh Arabi³ · Saeed Mohammadi^{2,4} · Yaghoob Yazdani^{2,4}

Received: 12 January 2019 / Accepted: 28 July 2019 / Published online: 20 August 2019
© Springer Nature Switzerland AG 2019

Abstract

Background *Leflunomide* (LFD) is an *Aryl hydrocarbon receptor* (AhR) agonist and immunomodulatory drug with several side effects. Niosomes are novel drug delivery systems used to reduce the unfavorable effects of drugs by enhancing their bioavailability, controlling their release and targeting specific sites.

Objectives Here, we prepared niosomal formulations of LFD, evaluated their properties and delivered to THP-1 monocytic cells to study the activation and nuclear translocation of AhR.

Methods Four types of non-ionic surfactants were utilized to formulate niosomes by thin film hydration (TFH) method. Entrapment efficiency (EE %) of niosomes were quantified and dynamic light scattering (DLS) was performed. Transmission electron microscopy (TEM) was used to identify the morphology of LFD niosomes. Dialysis method was used to measure LFD release rate. MTS assay was adopted to examine the viability of the cells upon each treatment. The nuclear transfer of AhR was investigated by Immunocytochemistry (ICC). The mRNA expression of IL1 β and CYP1A1 were evaluated using quantitative RT-PCR.

Results Span 60: cholesterol (1:1) showed the highest EE% (70.00 ± 6.24), largest particles (419.00 ± 4.16 nm) and the best uniformity with the lowest PDI (0.291 ± 0.007). TEM micrographs of Span 60 (1:1) nanoparticles showed conventional spherical vesicles with internal aqueous spaces. The release rate of LFD from Span 60 (1:1) vesicles was slower. Although the viability of LFD niosome-treated THP-1 cells was decreased, they were associated with lower cytotoxic effects compared with the free LFD counterparts. Both free and niosomal LFD treatments intensified the nuclear translocation of AhR. The mRNA expression of CYP1A1 was overexpressed while IL1 β was downregulated in both free and niosomal LFD treated combinations.

Conclusion LFD encapsulation in Span 60: cholesterol (1:1) niosomal formulation could be introduced as a suitable vehicle of transferring LFD to THP-1 cells, with minimal cytotoxic effects, enhancing the AhR nuclear translocation and activation and inducing immunomodulatory properties.

Keywords Aryl hydrocarbon receptor (AhR) · Drug delivery · Leflunomide (LFD) · Niosome

✉ Yaghoob Yazdani
Yazdani@goums.ac.ir

¹ Department of Medical Biotechnology, School of Advanced Technologies in Medicine, Golestan University of Medical Sciences, Gorgan, Iran

² Infectious Diseases Research Center, Golestan University of Medical Sciences, Gorgan, Iran

³ Medical Cellular and Molecular Research Center, Golestan University of Medical Sciences, Gorgan, Iran

⁴ Stem Cell Research Center, Golestan University of Medical Sciences, Po.Box: 4934174611, Gorgan, Iran

Introduction

Leflunomide (LFD) is an isoxazole derivative with immunomodulatory and anti-inflammatory properties. It is regularly appointed for the treatment of autoimmune disorders and chronic inflammatory conditions such as rheumatoid arthritis (RA) and psoriatic arthritis [1]. Several molecular mechanisms have been attributed to the anti-inflammatory functions of LFD including the inhibition of dihydroorotate dehydrogenase (DHODH) mitochondrial enzyme which is involved in the rate limited step of de novo pyrimidine synthesis and inhibiting T cells proliferation [2]. Higher doses of LFD are

capable of blocking tyrosine kinases that result in the G0/G1 cell cycle arrest [3].

LFD is also known as an *Aryl hydrocarbon receptor* (AhR) agonist. However, the role of AhR in mediating the anti-inflammatory effects of LFD is not thoroughly investigated [4]. AhR is a ligand-dependent cytosolic receptor and transcription factor which is important for the removal of environmental and/or nutritional chemicals. Likewise, it plays a decisive role in imperative cellular mechanisms such as cell differentiation, immune response and other physiological and/or pathologic events [5, 6]. AhR could be activated by various ligands such as natural compounds, endogenous agonists, pharmaceutical agents and environmental toxins [7]. 2,3,7,8-tetrachlorodibenzo-p dioxin (TCDD) is known as the major AhR ligand which is believed to evoke inflammatory immune response, promoting cancer and autoimmunity by binding to dioxin response elements (DRE) or xenobiotic responsive elements (XRE) [8]. However, various AhR ligands have been introduced to possess anti-inflammatory effects including cruciferous vegetables-derived AhR agonists such as *indole-3-carbinole* (I3C) [9]. Therefore, AhR could be introduced as an encouraging therapeutic target for the treatment of inflammatory conditions and cancer and a possible mechanism by which LFD exerts its anti-inflammatory properties.

Although LFD is among the first therapeutic approaches for the treatment of RA with acceptable immunomodulatory potentials, its administration could be associated with several limitations such as clinical side-effects to the patients and improper solubility and permeability [10]. In order to reduce unfavorable effects of drugs, several delivery methods have been developed and employed including nanocarriers which act as a reservoir in protecting the drug, enhancing bioavailability, controlling drug release and targeting specific sites. These nanocarriers include polymer nanoparticles, metal base and lipid base carriers such as liposomes, micelles and niosomes [9]. Niosomes are formed from non-ionic surfactants as basic components and additives like cholesterol in aqueous media resulting in bilayer vesicles. Depending on the preparation method, they can be unilamellar or multilamellar [11]. Presence of cholesterol affects important properties of vesicles including stability, entrapment efficiency and membrane permeability. They have same conformation to liposomes which make them capable of entrapping both hydrophilic drugs in the aqueous core and hydrophobic drugs between the bilayers [12]. Numerous advantages such as greater stability than liposomes, easy handling, storage and modification, low toxicity and biodegradability, lower cost, high oral bioavailability and skin penetration made niosomes promising vehicles for drug delivery [13, 14].

In the present study, we aimed to prepare a suitable niosomal formulation to encapsulate and deliver LFD to THP-1 monocytic cells and evaluated the bioavailability and physicochemical properties of LFD-niosomal formulation for

AhR nuclear translocation and activation in comparison to free LFD.

Materials and methods

Reagents and materials

LFD was acquired from Santa Cruz Biotechnology (Santa Cruz, USA). Span 60, Span 20, Cholesterol, PMA (Phorbol 12-myristate 13-acetate), Tri Reagent RNA extraction and DAPI (4', 6-diamidino-2-phenylindole) were supplied by Sigma (Sigma-Aldrich, USA). Tween 20 and Tween 80 were purchased from Acros Organics (Morris Plains, USA). RPMI 1640, FBS (fetal bovine serum) and penicillin streptomycin (pen/strep) were obtained from Gibco (Life Technologies, USA). CDNA synthesis kit, primary (Anti-AhR antibody) and secondary (DyLight conjugated goat anti-rabbit IgG) antibodies were purchased from eBioscience (Thermo Fisher, USA). Real-time PCR SYBR green Master Mix was provided by Yekta Tajhiz Azma (Tehran, Iran). THP-1 monocytic cells were gently gifted by Dr. Shokri's laboratory (Immunology department, Tehran University of Medical Sciences). All used materials and solvents were prepared in analytical grades.

The procedure of preparing niosomes

A thin film hydration (TFH) method with minimal changes was optimized and applied to prepare niosomes [11]. Different molar ratios (1:1, 2:1) of non-ionic surfactants (Tween 20, Tween 80, Span 60 and Span 20) and cholesterol with a selected concentration of LFD were accurately weighed and dissolved in an organic solvent (ethanol: chloroform [1:1 v/v]). The solution was then dried up at 37 °C, and the formed thin film was hydrated in phosphate buffered saline (PBS), pH 7.4. The suspension was firmly shaken at 60 °C for 45 min and then kept in 25 °C for 16–18 h to allow complete partitioning of the drug between bilayers. The resulting suspension was centrifuged for 10 min at 2000 rpm and sonicated in a bath-sonicator for 10 min with 2-min interval.

Quantifying entrapment efficiency (EE %)

We performed a centrifugation method to separate niosome-entrapped LFD from the free LFD, as previously described by Uchegbu et al. with a little modification [15]. Niosomal suspension was centrifuged at 15000 rpm at 4 °C for 1 h. The pellet was washed with PBS pH 7.4 and recentrifuged for complete separation of the free LFD. The niosomal pellet was dissolved in ethanol, vortexed and the amount of entrapped LFD was determined by spectrophotometry at the wavelength of 260 nm.

The entrapment efficiency was quantified using the following formulation:

$$\text{LFD\%EE} = \frac{\text{amount of LFD entrapped}}{\text{total amount of LFD}} \times 100$$

Determination of zeta potential and niosomal particle size

The samples were transferred to the pharmacology laboratory of Mazandaran University of Medical Sciences, Sari, Iran. The zeta potential, the size of niosomal particles and polydispersity index (PDI) of the vesicles were estimated dynamic light scattering (DLS) (Zetasizer Nano ZS; Malvern Instruments, Malvern, UK) at 25.0 ± 0.1 °C.

The release rate of LFD from niosomal vesicles

The in vitro release rate of LFD was measured by dialysis method [16]. Briefly, a 12 KDa MWCO dialysis bag soaked in warm water for 10 min. The niosomal suspensions (2 ml) were transferred to the dialysis bag and were tightly fixed from both ends to prevent leakage and suspended to 50 ml of PBS; pH 7.4. The medium was then stirred at 100 rpm, 37 ± 2 °C. Samples were taken from medium in determined time intervals, replaced with fresh buffer, replenished with the same volume of fresh fluid and measured spectrophotometrically at the maximum wavelength of 260 nm.

Characterizing the morphology of niosomes

The morphology of LFD niosomes were defined by transmission electron microscopy (TEM). A 20 μL droplet of the niosomal preparation was located on a carbon film coated on 300 netting copper grid (Agar) for 2 min. The extra liquid was removed by a filter paper and counter-stained with 20 μL of uranyl acetate (2%) for 2 min. The overflow liquid was washed away and the layer was allowed to air dry. Grids were then analyzed under a Zeiss EM10C TEM operating at an accelerating voltage of 100 kV.

Cellular viability test

THP-1 monocytic cell line was cultured in RPMI-1640 medium supplemented with 10% FBS, 1% pen/strep in a 95% humidified incubator with 5% CO₂ at 37 °C. PMA treatment was conducted to access balanced expression of AhR in THP-1 cells [17]. PMA treated cells were then seeded in 96-well tissue culture-treated plate at a density of $1.5\text{--}2 \times 10^4$ cells per well. The cells were treated with different concentration of LFD and LFD-loaded niosomes (1, 10, 50 and 100 μM) for 24 h, 48 h and 72 h.

The viability of the cells were assessed by MTS (3-(4,5-dimethylthiazol-2-yl)-5-(3-carboxymethoxyphenyl)-2-(4-sulfophenyl)-2H-tetrazolium) assay [18]. MTS solution was added to each well after accomplishing each treatment, incubated for 3–4 h at 37 °C and the absorbance were obtained at the wavelength of 490 nm in a microplate photometer (Awareness Technology ChroMate® Micro plate Reader).

Immunocytochemistry (ICC) staining

THP-1 macrophage-like cells were cultured in 6-well tissue culture-treated plates (5×10^5 cells/ml) after each treatment, fixed with 4% paraformaldehyde, washed with PBS and soaked in 0.1% Triton X-100 for 15 min to increase the cells permeability. In order to reduce nonspecific bindings, PBS/BSA 1% was used as a blocking solution. As primary antibody, anti-AhR monoclonal antibody was added and after incubation and washing, staining performed with secondary antibody. In this process different aspects about antibody-antigen interaction were considered [19]. The cell staining was completed with DAPI. Finally cells were observed and imaged with a florescent microscope (Nikon, Eclipse Ti) and the nuclear translocation of AhR was measured using Image J (<http://rsbweb.nih.gov/ij>) [20].

RNA isolation and quantitative real-time PCR

Total RNA was extracted using Tri Reagent following the protocols provided by the manufacturer. The quality and quantity of RNA was evaluated using Picodrop (Picodrop limited, Walden, UK). Synthesis of cDNA was performed using 1 μg of extracted total RNA. LineGene K qPCR apparatus (Bioer Technology, China) was used to perform cDNA amplification using SYBR Green PCR Master Mix. The 18srRNA housekeeping gene was used for normalizing the expression level and agarose gel electrophoresis was used to verify the accuracy of PCR amplifications. The oligonucleotide primer pairs were designed and evaluated to expand exon junctions. The sequences of gene specific primers are listed in Table 1.

Statistical analyses

All of the examinations were conducted in triplicates and the data were represented as means \pm SD (standard deviation). SPSS 22.0 (SPSS Inc., Chicago, IL) was utilized to perform statistical analyses and graphical charts were depicted using Graphpad Prism 5.04 (GraphPad Software, La Jolla, CA). In order to compare the means of different variables, one-way ANNOVA with *tukey* post-test was implemented. *P*-values smaller than 0.05 were considered to be significant.

Table 1 Gene specific primers

Primer (accession)	Sequence (5' > 3')	t_m	Amplicon size
CYP1A1 (NM_000499)	F: TCCTGGAGCCTCATGTATT R: TCTCTTGTGTGCTGTGG	61	200 bp
IL1 β (NM_000576)	F: GGCTTATTACAGTGGCAATG R: TAGTGGTGGTCGGAGATT	60	135 bp
18srRNA (M10098)	F: CAGCCACCCGAGATTGAGCA R: TAGTAGCGACGGGCGGTGTG	61	252 bp

Results

Entrapment or encapsulation efficiency (EE %) of LFD

Four types of non-ionic surfactants including Tween 20, Tween 80, Span 20 and Span 60 were utilized to prepare niosomal vesicles by TFH method. Niosomes were then characterized according to their physical and/or chemical properties (Table 2). To obtain the most proper EE %, two aspects including the structure of the surfactants and the cholesterol balance were optimized (Fig. 1). The EE % of Span 60-prepared niosomes was generally higher than those prepared with Span 20. Although the EE % of Tween 80 was higher than Tween 20, the EE% of Span 60 represented the greatest EE% (70.00 ± 6.24) among all preparations and was selected for the construction of niosomal constructions at the molar ratio of 1:1 with cholesterol.

In vitro release study of LFD

Figure 2 represents the release rate of LFD from niosomal preparations of Span 60 and cholesterol (1:1 ratio) in comparison to the free LFD in different time-points. The release rate of LFD from niosomal vesicles was slower compared with free drug. After 5 h, $91.41 \pm 1.06\%$ of free LFD was released, whereas only 44.56 ± 2.79 of LFD was leaked from niosomal preparations (Fig. 2).

Table 2 Characterization of nanoparticles; size, entrapment efficiency, zeta potential and PDI of each niosomal composition

Surfactant	EE%		Size (nm)	Zeta potential (-mV)	PDI
	Cholesterol: Surfactant ratio				
	1:1	1:2			
Span 20	62.00 ± 4.36	22.00 ± 2.00	267.33 ± 20.98	17.00 ± 1.05	0.316 ± 0.005
Span 60	70.00 ± 6.24	30.00 ± 5.29	419.00 ± 4.16	12.2 ± 4.99	0.291 ± 0.007
Tween 20	37.00 ± 3.61	28.00 ± 2.65	198.33 ± 7.10	3.53 ± 0.84	0.436 ± 0.008
Tween 80	44.66 ± 4.16	11.00 ± 2.65	205.00 ± 14.80	3.87 ± 0.25	0.633 ± 0.153

EE: entrapment efficiency; PDI: poly dispersity index. Data are shown as the mean \pm SD ($N = 3$)

Physical properties and the surface morphology of niosomal preparations

As shown in Table 2, three physical properties of all prepared niosomes including the size of particles, polydispersity index (PDI) and zeta potential were evaluated (Table 2). The sizes of niosomal vesicles as obtained by DLS ranged from 198.33 ± 7.10 nm in Tween 20 to 419.00 ± 4.16 nm in Span 60. Span 60- and Tween 80-prepared niosomes were larger in size in comparison to Span 20 and Tween 20 nanocarriers, respectively. The lowest zeta potential was observed in Tween 20 niosomal formulations (3.53 ± 0.84), while the highest zeta potential was shown in Span 20 formulations (17.00 ± 1.05). The PDI shows the consistency of the vesicle size in the niosomal preparation [21, 22]. Accordingly, Span 60 with the lowest PDI (0.291 ± 0.007) showed the best uniformity and was selected for further experiments at the molar ratio of 1:1 to cholesterol. In order to evaluate the surface morphology of niosomal formulations, a transmission electron microscopy (TEM) was conducted which showed the conventional spherical vesicles with internal aqueous spaces (Fig. 3).

The cytotoxic effects of niosomal LFD was minimal on THP-1 cells

The cytotoxicity effects of niosomal LFD was evaluated in comparison to free LFD using MTS assay. As depicted in

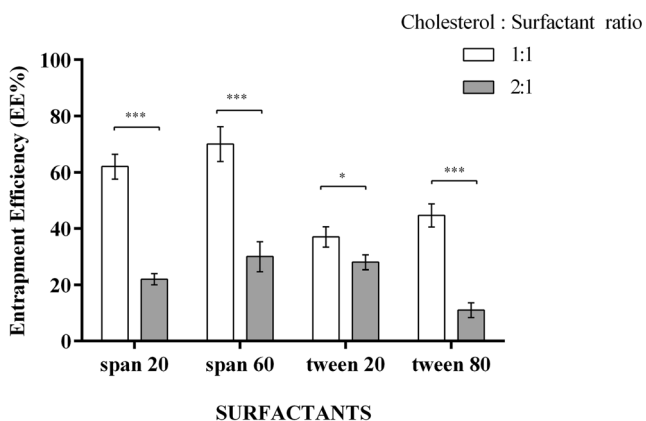


Fig. 1 Entrapment efficiency of LFD with differing ratios of surfactants: cholesterol; the EE% of Spans were significantly higher than Tweens. The ratio of Span 60: Cholesterol (1:1) was chosen with the greatest significant EE%. Each bar represents means ± SD (standard deviation) of a single experiment with three replicates. One-way ANNOVA with Tukey *post-test* was carried out to compare more than two groups. * $P < 0.05$, *** $P < 0.001$

Fig. 4a, a significant decline was demonstrated in the viability of THP-1 cells upon 24 h of treatment with higher concentrations of free LFD (50 μM and 100 μM free LFD). However, niosomal LFD exerted no cytotoxic effects at the mentioned time point with the treated concentrations. Similarly, the percentages of viable THP-1 cells have significantly decreased upon treatment with higher concentrations of free LFD after 48 h (Fig. 4b) and 72 h (Fig. 4c). Although the viability of THP-1 cells treated with higher levels of niosomal LFD was declined in a time- and dose- dependent manner, they were associated with lower cytotoxic effects in comparison to the free LFD counterparts.

Immunocytochemistry (ICC) staining of AhR and quantification of its nuclear translocation

LFD is known as a potential AhR agonist. In order to visualize and quantify the cytosolic expression and AhR translocation

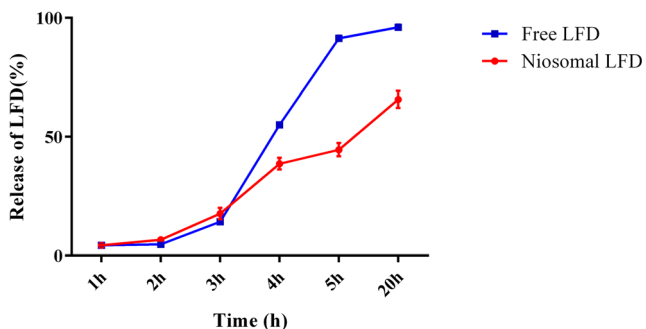


Fig. 2 The release rate (in vitro) of LFD from niosomal vesicles of Span 60 and cholesterol (1:1) in PBS (pH 7.4); the release rate of drug from niosomal vesicles was slower in comparison to the free LFD. After 5 h, $91.41 \pm 1.06\%$ of free LFD was released, while $44.56 \pm 2.79\%$ of LFD was leaked. All values are demonstrated as mean ± standard deviation ($N = 3$)

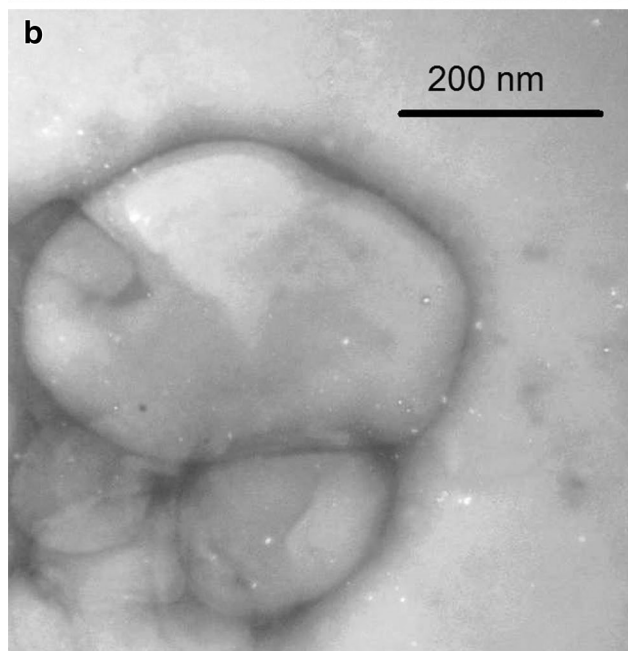
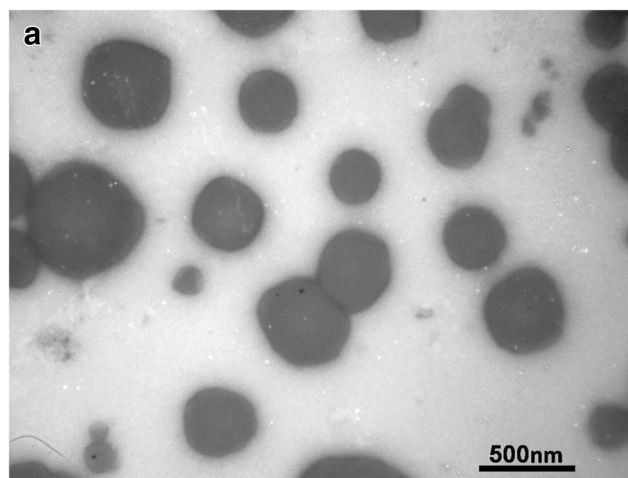


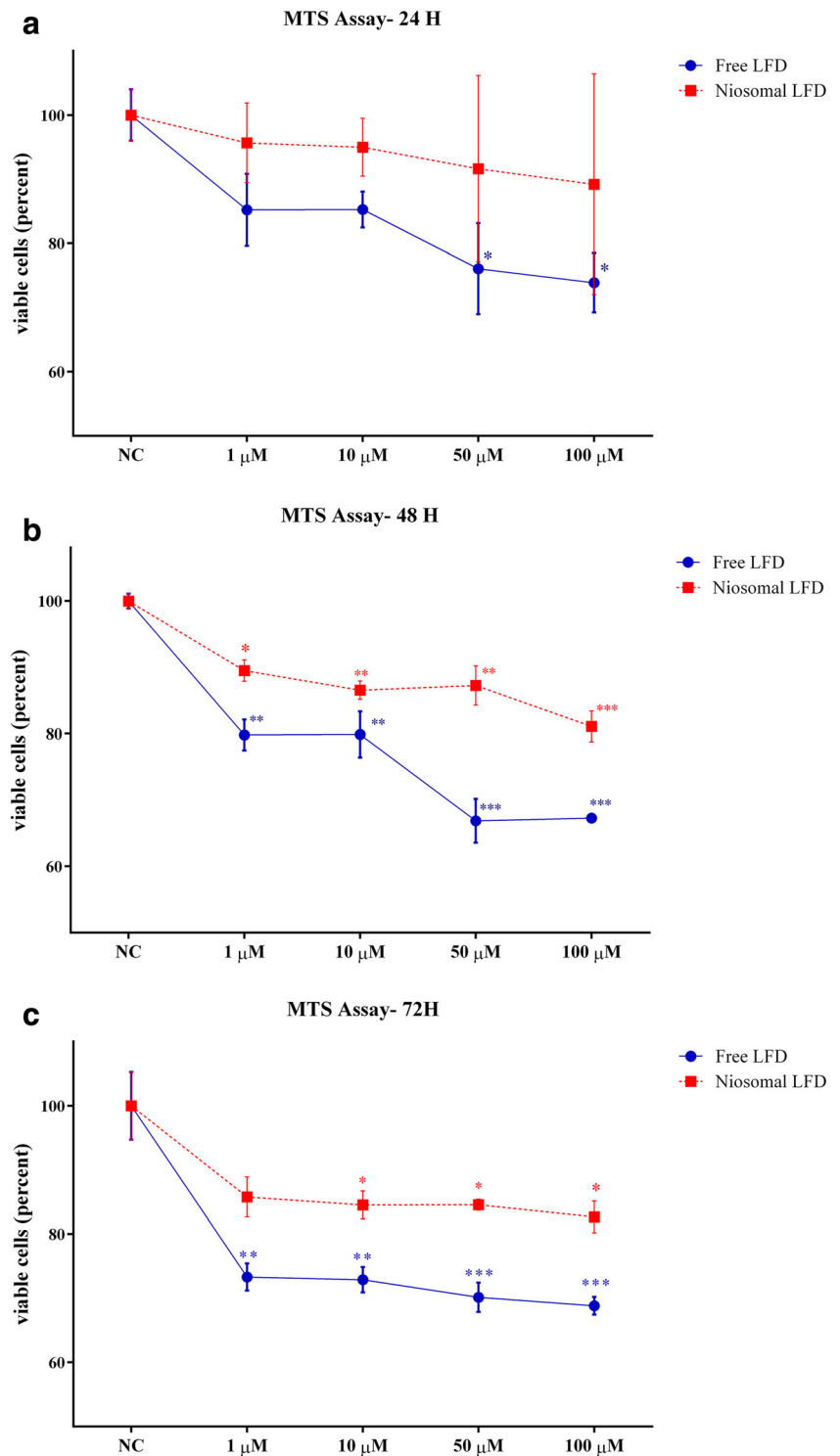
Fig. 3 TEM morphology of the optimized LFD niosomes; TEM was utilized to characterize the morphology of Span 60 niosomal vesicles and showed conventional spherical vesicles with internal aqueous spaces. Scale bars (a 500 nm; b 200 nm)

to the nuclei, an ICC staining followed by florescent microscopy was applied. As shown in Fig. 5, both free and niosomal LFD enhanced the displacement of AhR to the nuclei of THP-1 cells and the niosomal formulation of LFD was efficient enough for AhR activation.

The activation and expression status of AhR target genes

The mRNA expression of CYP1A1 was used to validate the proper AhR activation upon LFD treatment in both forms. Moreover, the mRNA expression of pro-inflammatory IL1β which is regulated by AhR was quantified. The

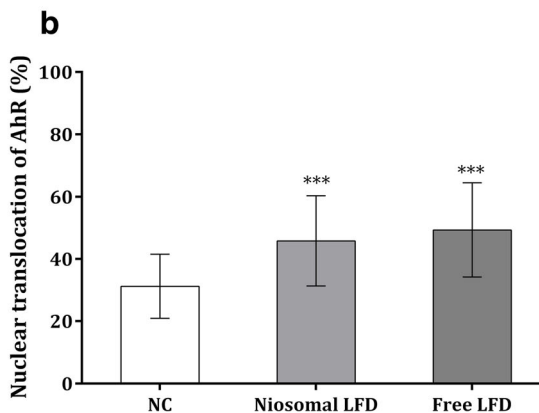
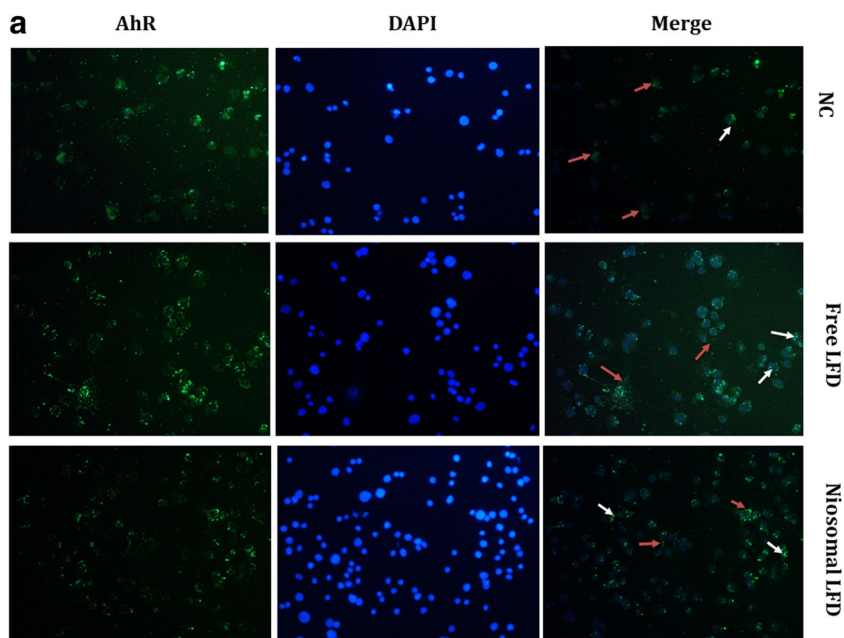
Fig. 4 Minimal cytotoxic effects of LFD niosomal vesicles on THP-1 cells; THP-1 cells were treated with different concentrations of LFD (1 μ M, 10 μ M, 50 μ M and 100 μ M) for 24 (a), 48 h (b) and 72 h (c). The cell viability of all treatments were evaluated by MTS assay. Free LFD showed compelling cytotoxicity effects on THP-1 cells. The niosomal composition of LFD exerted minimum toxicity in all time points. NC: negative control (non-treated cells). Data represented the mean \pm SE (standard error) from three independent replicates. The means of different experiments were compared using one-way ANNOVA and Tukey's *post-test*. The significant level: 0.05 * P < 0.05, ** P < 0.01, *** P < 0.001



CYP1A1 level was markedly increased in LFD-treated THP-1 samples compared with the non-treated counterparts. Moreover, CYP1A1 was significantly overexpressed in niosomal LFD-treated group compared with the free LFD combination (Fig. 6a). IL1 β was significantly down-

regulated in both niosomal and free LFD-treated THP-1 cells compared with the no-treated combinations (Fig. 6b). However, no difference was demonstrated between the expression of IL1 β in niosomal and free LFD-treated samples (Fig. 6b).

Fig. 5 The cytoplasmic (Red arrows) and nuclear expression (White arrows) of AhR in free LFD and niosomal LFD-treated cells; translocation of AhR was shown in both treatments. The fluorescent signal of the isotype control (secondary antibody) was compensated in quantitative analysis. DAPI-stained nuclei (Blue) were merged with green-fluorescent emission of AhR-positive cells (40X magnification) (a). Image J was utilized for data quantification in each combination (b). NC: negative control (non-treated cells). Each bar demonstrated the mean \pm SD (standard deviation) from three experiments. One-way ANNOVA with Tukey post-test was carried out to compare more than two groups. *P*-values greater than 0.05 presumed to be not significant. ****P* < 0.001



Discussion

In order to efficiently introduce drugs to the cellular targets with minimal side-effects, several delivery systems have been developed including nanocarriers such as liposomes and niosomes [23]. Niosomes are stable and biodegradable bilayer vesicles formed of non-ionic surfactants and additives such as cholesterol in an aqueous phase with enhanced stability, entrapment efficiency and membrane permeability [24]. *Aryl hydrocarbon receptor* (AhR) is a ligand-dependent transcription factor and receptor [25, 26] that is involved in detoxification of environmental toxins, numerous cellular functions and immunoregulatory effects [27, 28]. It is activated by a diverse range of chemicals, while several agonists and antagonists have been attributed in this regard. *Leflunomide* (LFD) is an anti-inflammatory and immunomodulatory drug used for the treatment of chronic inflammatory disorders [1]. Several molecular mechanisms have been introduced to be involved in the anti-inflammatory properties of LFD [29]. However, as an AhR agonist, the role of AhR signaling pathway in the

immunomodulatory functions of LFD is not completely studied [4]. Here, we encapsulated LFD in a niosomal formulation and characterized according to its physicochemical properties. We also studied the viability of THP-1 cells upon treatment with free and niosomal LFD, and quantified the translocation of AhR to the cellular nuclei and their activation in each combination.

Four types of surfactants were used for the construction and optimization of niosomes according to the structure of the surfactants and their molar ratio to cholesterol. The EE% of Spans were basically higher than Tweens and Span 60 (1:1) with the EE% of 70.00 ± 6.24 was selected for the preparation of LFD niosomal formulations and further in vitro investigations. The higher entrapment efficiency among Spans could be attributed to the structure of these surfactants. Tween 20 and Tween 80 have the same head group but Tween 80 has a longer saturated alkyl chain and lower hydrophilic-lipophilic balance (HLB) than Tween 20 with higher entrapment efficiency [14]. Similar to Tweens, Span 60 has a longer saturated alkyl chain and lower HLB than Span 20 and higher EE %.

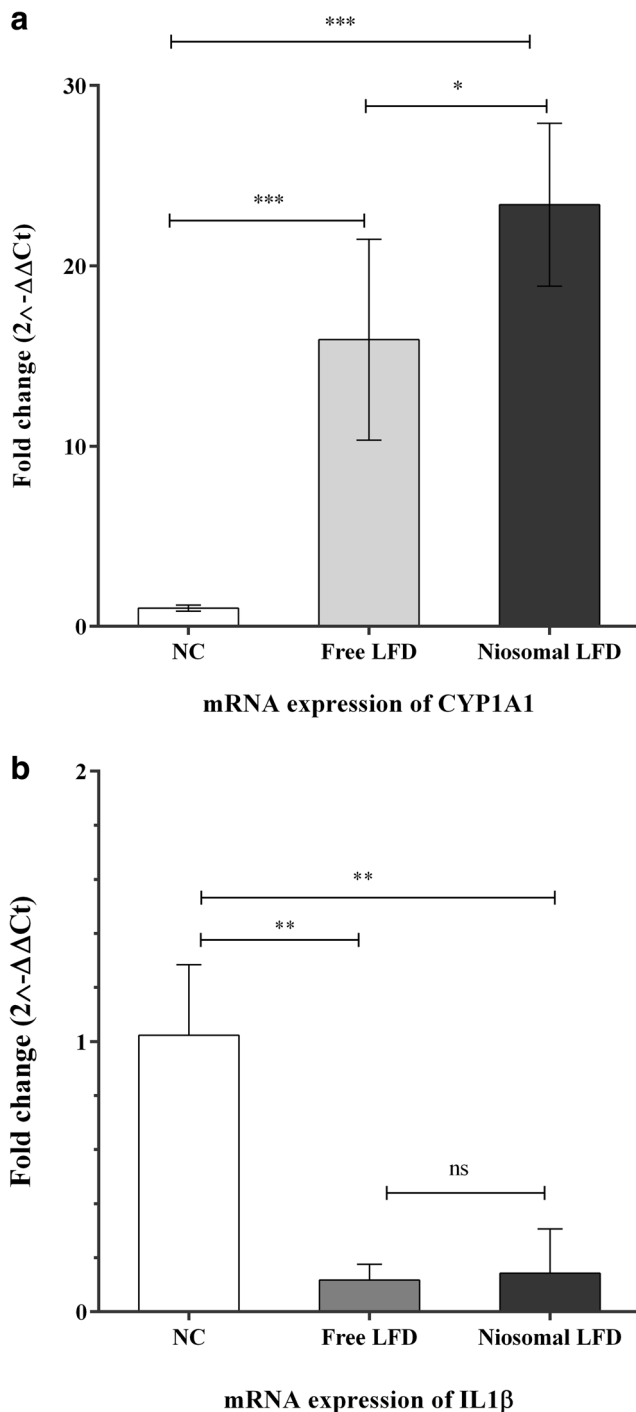


Fig. 6 The mRNA expression of IL1 β and CYP1A1 upon treatments with free and niosomal LFD; CYP1A1 was increased in response to both free LFD and niosomal treatments (a). IL1 β was downregulated in both niosomal and free LFD-treated cells (b). $2^{-\Delta\Delta Ct}$ method was used to quantify the mRNA expression in comparison to the expression of non-treated combinations (The fold change was promptly set at 1 for NC). Each bar represented the mean \pm SD (standard deviation) from three replicates. One-way ANNOVA with Tukey *post-test* was carried out to compare more than two groups. *P*-values <0.05 were assumed as significant quantities. *******P* <0.01 , ********P* <0.001 . NS: not significant

The elongated alkyl chain affects the HLB value of the surfactant mixture which literally modulates the drug EE % [30]. These results are comparable to the results reported by Ahmed et al. [31] and discordance with the results reported for zidovudine niosomes [14]. This discrepancy with the previous findings could be due to the drug properties such as their solubility which affects the placement of chemicals in the niosome. Regarding the molar ratio of surfactants to the content of cholesterol, niosomes with equimolar ratios of cholesterol and surfactant could entrap more quantities of LFD than those with molar ratios of 1:2 cholesterol and surfactant. Cholesterol increased the entrapment efficiency of niosomal formulations due to its ability of increasing the viscosity which results in more rigidity of the membrane. Cholesterol is capable of acting as a bilayer cement which could prevent the leakage of the entrapped chemical drugs [32]. These findings were comparable to the results reported on niosomal colchicine [32]. As depicted in Fig. 2, the release rate of LFD from niosomal vesicles was slower compared with free LFD. These findings revealed that our niosomal vesicles could control the release of LFD compared with the free drug and could be introduced as promising vesicles to reduce the unwanted side effects of LFD.

DLS experiments on physical characteristics of prepared niosomes revealed that the size of niosomes were affected by the surfactant type. Niosomes prepared with Span 60 and Tween 80 represented larger vesicles in comparison to Span 20 and Tween 20 nanocarriers. These effects are probably due to the elongated alkyl chain of surfactants. Span 60 and Tween 80 which possess longer alkyl chains formed larger vesicles than Span 20 and Tween 20 respectively [24]. A positive correlation between the EE% (1:1) and vesicles size is also noticeable. The larger the vesicle (Span 60 > Span 20 > Tween 80 > Tween 20), the higher the EE% (Span 60 > Span 20 > Tween 80 > Tween 20). Although the zeta potentials of all prepared formulations did not exceed 20 due to not using compounds such as *dicetyl phosphate* (DCP), the highest zeta potential was shown in Span 20 formulations, even in comparison to Span 60. It should be noticed that hydrophilicity of Span 20 (HLB: 8.6) is higher than Span 60 (HLB: 4.7), hence niosomes with higher hydrophilicity represent higher zeta potential values [33]. The PDI index shows the uniformity of the vesicle size in niosomal preparations [21, 22]. Span 60 (1:1) with lowest PDI showed best uniformity and with the most proper vesicle size and acceptable zeta potential was selected for further experiments. The Span 60 niosomal preparations of LFD represented conventional spherical vesicles with internal aqueous spaces under TEM microscopic evaluations and confirmed to be employed for the treatment of THP-1 cells and studying AhR activation.

The MTS cytotoxicity results showed a dose- and time-dependent decline in the viability of THP-1 cells upon LFD treatments. However, niosomal LFD exerted minimal cytotoxic effects in comparison to the free LFD counterparts. These findings indicate that the niosomal formulation of LFD could be associated with lower cytotoxic effects and this formulation could be employed for the experiments which need higher safety levels and viability of the cells. It has been reported that LFD could activate AhR as an AhR agonist [4, 34]. In order to monitor the nuclear translocation of AhR, an ICC staining method was applied. Both free and niosomal LFD promoted the nuclear translocation. Finally, the mRNA levels of CYP1A1 and IL1 β were used to establish the proper activation of AhR and studying the immunomodulatory effects of this activation upon LFD treatment in THP-1 cells. CYP1A1 was significantly overexpressed in LFD-treated THP-1 cells, in which the niosomal formulations represented higher levels of CYP1A1. The pro-inflammatory IL1 β was down-regulated in both niosomal and free LFD-treated groups and demonstrated no significant difference between these two treatment groups. Therefore, Span 60: cholesterol (1:1) niosomal LFD is capable of activating AhR after enhancing its nuclear translocation and is associated with anti-inflammatory properties by downregulating the expression of pro-inflammatory IL1 β .

Conclusion

Span 60: cholesterol (1:1) niosomal formulation with the highest entrapment efficiency, the most convenient *in vitro* release rate, the most proper particle size and lowest PDI was selected for the construction of niosomes and LFD encapsulation. Niosomal LFD was associated with lower cytotoxic impacts on THP-1 cells and was capable of efficient translocation of AhR to the nucleus. Although both free and niosomal LFD increased the mRNA expression of CYP1A1, niosomal LFD was more successful in AhR activation. LFD (in both niosomal and free forms) was capable of inducing anti-inflammatory effects on THP-1 cells by reducing the mRNA levels of IL1 β . Therefore, encapsulation of LFD in a Span 60: cholesterol (1:1) niosomal formulation could be introduced as a suitable vehicle of transferring LFD to THP-1 cells, enhancing the AhR nuclear translocation and activation and inducing immunomodulatory effects. However, further *in vitro* and *in vivo* experimental studies are suggested to determine and confirm the anti-inflammatory effects of LFD in its niosomal formulation and studying alterations in the side-effects of LFD.

Acknowledgments This article was derived from a thesis of M.Sc. degree in the field of Medical biotechnology (Grant Number: 960129002) at Gorgan School of Advanced Technologies in Medicine of Golestan University of Medical Sciences, Gorgan, Iran. We would like to thank Dr. Samadian, Mrs. Yousefi and Mrs. Haydari for their scientific and technical support.

Author contributions MH: Acquisition of data, Analyses and interpretations of data, Manuscript drafting, Revision of the manuscript. NAS: Participation in data acquisition, analyses and interpretations. MSA: Participation in data acquisition. BK: Participation in data acquisition. SM: Study design and concept, participation in literature bibliography, data acquisition and analysis, manuscript drafting and critical revision of the manuscript. YY: Participation in study design and final revision of the manuscript. All authors read and approved the final version of the manuscript.

Data availability Datasets analyzed during the present research study would be available from the corresponding author on request.

Compliance with ethical standards

Conflict of interests On behalf of all authors, the corresponding author states that there is no conflict of interest.

Consent for publication Not applicable.

Ethics approval and consent to participate The study was approved by the Ethics committee of Golestan University of Medical Sciences (Code of Ethics: IR.GUOMS.REC.13950259).

References

1. Frago YD, Brooks JBB. Leflunomide and teriflunomide: altering the metabolism of pyrimidines for the treatment of autoimmune diseases. *Expert Rev Clin Pharmacol*. 2015;8(3):315–20.
2. Fox RI, Herrmann ML, Frangou CG, Wahl GM, Morris RE, Strand V, et al. Mechanism of action for leflunomide in rheumatoid arthritis. *Clin Immunol*. 1999;93(3):198–208. <https://doi.org/10.1006/clin.1999.4777>.
3. Cutolo M, Sulli A, Ghiorzo P, Pizzorni C, Cravio C, Villaggio B. Anti-inflammatory effects of leflunomide on cultured synovial macrophages from patients with rheumatoid arthritis. *Ann Rheum Dis*. 2003;62(4):297–302.
4. O'Donnell EF, Saili KS, Koch DC, Kopparapu PR, Farrer D, Bisson WH, et al. The anti-inflammatory drug leflunomide is an agonist of the aryl hydrocarbon receptor. *PLoS One*. 2010;5(10):e13128.
5. Baban B, Liu JY, Mozaffari MS. Aryl hydrocarbon receptor agonist, leflunomide, protects the ischemic-reperfused kidney: role of Tregs and stem cells. *Am J Physiol Regul Integr Comp Physiol*. 2012;303(11):R1136–R46.
6. Yazdani Y, Sadeghi H, Alimohammadian M, Andalib A, Moazen F, Rezaei A. Expression of an innate immune element (mouse hepcidin-1) in baculovirus expression system and the comparison of its function with synthetic human hepcidin-25. *Iran J Pharm Res*. 2011;10(3):559–68.

7. Jutooru I, Chadalapaka G, Safe S. Aryl hydrocarbon receptor ligands: toxic, biochemical, and therapeutic effects. *Endocrine toxicology*. 3rd ed. Boca Raton, Florida, United States: CRC Press; 2016. p. 201–21.
8. Vondracek J, Umannova L, Machala M. Interactions of the aryl hydrocarbon receptor with inflammatory mediators: beyond CYP1A regulation. *Curr Drug Metab*. 2011;12(2):89–103.
9. Tilg H. Cruciferous vegetables: prototypic anti-inflammatory food components. *Clin Phytosci*. 2015;1(1):10.
10. Pund S, Pawar S, Gangurde S, Divate D. Transcutaneous delivery of leflunomide nanoemulgel: mechanistic investigation into physicochemical characteristics, in vitro anti-psoriatic and anti-melanoma activity. *Int J Pharm*. 2015;487(1):148–56.
11. Waddad AY, Abbad S, Yu F, Munyendo WL, Wang J, Lv H, et al. Formulation, characterization and pharmacokinetics of Morin hydrate niosomes prepared from various non-ionic surfactants. *Int J Pharm*. 2013;456(2):446–58.
12. Hong M, Zhu S, Jiang Y, Tang G, Pei Y. Efficient tumor targeting of hydroxycamptothecin loaded PEGylated niosomes modified with transferrin. *J Control Release*. 2009;133(2):96–102.
13. Moghassemi S, Hadjizadeh A. Nano-niosomes as nanoscale drug delivery systems: an illustrated review. *J Control Release*. 2014;185:22–36.
14. Ruckmani K, Sankar V. Formulation and optimization of zidovudine niosomes. *AAPS PharmSciTech*. 2010;11(3):1119–27.
15. Uchegbu IF, Duncan R. Niosomes containing N-(2-hydroxypropyl) methacrylamide copolymer-doxorubicin (PK1): effect of method of preparation and choice of surfactant on niosome characteristics and a preliminary study of body distribution. *Int J Pharm*. 1997;155(1):7–17.
16. Akbarzadeh A, Rezaei-Sadabady R, Davaran S, Joo SW, Zarghami N, Hanifehpour Y, et al. Liposome: classification, preparation, and applications. *Nanoscale Res Lett*. 2013;8(1):102.
17. Daigneault M, Preston JA, Marriott HM, Whyte MK, Dockrell DH. The identification of markers of macrophage differentiation in PMA-stimulated THP-1 cells and monocyte-derived macrophages. *PLoS One*. 2010;5(1):e8668.
18. Yazdani Y, Keyhanvar N, Kalhor HR, Rezaei A. Functional analyses of recombinant mouse hepcidin-1 in cell culture and animal model. *Biotechnol Lett*. 2013;35(8):1191–7.
19. Roohi A, Yazdani Y, Khoshnoodi J, Jazayeri SM, Carman WF, Chamankhah M, et al. Differential reactivity of mouse monoclonal anti-HBs antibodies with recombinant mutant HBs antigens. *World J Gastroenterol*. 2006;12(33):5368–74.
20. Schneider CA, Rasband WS, Eliceiri KW. NIH image to ImageJ: 25 years of image analysis. *Nat Methods*. 2012;9(7):671–5.
21. Danaei M, Dehghankhold M, Ataei S, Hasanzadeh Davarani F, Javanmard R, Dokhani A, et al. Impact of particle size and polydispersity index on the clinical applications of lipidic nanocarrier systems. *Pharmaceutics*. 2018;10(2):57.
22. Bera B, editor. Nanoporous silicon prepared by vapour phase strain etch and sacrificial technique. *Proceedings of the International Conference on Microelectronic Circuit and System (Micro)*, Kolkata, India; 2015.
23. Tibbitt MW, Dahlman JE, Langer R. Emerging frontiers in drug delivery. *J Am Chem Soc*. 2016;138(3):704–17.
24. Abdelbary G, El-gendy N. Niosome-encapsulated gentamicin for ophthalmic controlled delivery. *AAPS PharmSciTech*. 2008;9(3):740–7.
25. Nebert DW, Dalton TP, Okey AB, Gonzalez FJ. Role of aryl hydrocarbon receptor-mediated induction of the CYP1 enzymes in environmental toxicity and cancer. *J Biol Chem*. 2004;279(23):23847–50.
26. Murray IA, Patterson AD, Perdew GH. Aryl hydrocarbon receptor ligands in cancer: friend and foe. *Nat Rev Cancer*. 2014;14(12):801–14.
27. Faust D, Kletting S, Ueberham E, Dietrich C. Aryl hydrocarbon receptor-dependent cell cycle arrest in isolated mouse oval cells. *Toxicol Lett*. 2013;223(1):73–80.
28. Stockinger B, Meglio PD, Gialitakis M, Duarte JH. The aryl hydrocarbon receptor: multitasking in the immune system. *Annu Rev Immunol*. 2014;32:403–32.
29. Li EK, Tam LS, Tomlinson B. Leflunomide in the treatment of rheumatoid arthritis. *Clin Ther*. 2004;26(4):447–59.
30. Raja NR, Pillai G, Udupa N, Chandrashekar G. Anti-inflammatory activity of niosome encapsulated diclofenac sodium in arthritic rats. *Indian J Pharmacol*. 1994;26(1):46.
31. Guinedi AS, Mortada ND, Mansour S, Hathout RM. Preparation and evaluation of reverse-phase evaporation and multilamellar niosomes as ophthalmic carriers of acetazolamide. *Int J Pharm*. 2005;306(1):71–82.
32. Marwa A, Omaima S, Hanaa E-G, Mohammed A-S. Preparation and in-vitro evaluation of diclofenac sodium niosomal formulations. *Int J Pharm Sci Res*. 2013;4(5):1757–65.
33. Zaki RM, Ali AA, El Menshawe SF, Bary AA. Formulation and in vitro evaluation of diacerein loaded niosomes. *Int J Pharm Pharm Sci*. 2014;6(Suppl 2):515–21.
34. Hu W, Sorrentino C, Denison MS, Kolaja K, Fielden MR. Induction of Cyp1a1 is a non-specific biomarker of aryl hydrocarbon receptor activation: results of large scale screening of pharmaceuticals and toxicants in vivo and in vitro. *Mol Pharmacol*. 2007;71(6):1475–86.

Publisher's note Springer Nature remains neutral with regard to jurisdictional claims in published maps and institutional affiliations.